月旦知識庫

Bio-inspired chitosan/polydopamine-nanoparticle based sorbent bead: A versatile platform for separation and HPLC analysis of tetracycline antibiotics from various sample matrix

Emmanuvel Arputharaj [a], Yu-Hui Huang [a], Shivangi Singh [a], Chen-Han Zhuang [a], Kuei-Ying Lin [b], Sri Sudewi [c], You-Rong Wu [a], Yeou-Lih Huang [a,d,e,f,g,*]

[a] Department of Medical Laboratory Science and Biotechnology, Kaohsiung Medical University, Kaohsiung, Taiwan
[b] Department of Laboratory Medicine, Municipal Ta-Tung Hospital, Kaohsiung Medical University Hospital, Kaohsiung Medical University, Kaohsiung, Taiwan
[c] Department of Pharmacy, Faculty of Mathematics and Natural Science, Universitas Sam Ratulangi, Manado, Indonesia
[d] Research Center for Precision Environmental Medicine, Kaohsiung Medical University, Kaohsiung, Taiwan
[e] Department of Medical Research, Kaohsiung Medical University Hospital, Kaohsiung Medical University, Kaohsiung, Taiwan
[f] College of Professional Studies, National Pingtung University of Science and Technology, Pingtung, Taiwan
[g] Department of Chemistry, National Sun Yat-Sen University, Kaohsiung, Taiwan

Abstract

This study introduces an innovative bio-based sorbent bead crafted by integrating chitosan (CS) biopolymers, $Fe(NO_3)_3$ and polydopamine nanoparticles (PDA NPs) via glutaraldehyde crosslinking. The primary focus of this study was the concurrent separation of diverse tetracycline antibiotics (TCs), followed by rigorous reversed-phase liquid chromatography analysis. The fabricated CS/Fe@PDA sorbent beads were comprehensively characterized using scanning electron microscopy and energy-dispersive X-ray spectroscopy, revealing a surface rich in active carbon (C), nitrogen (N), and oxygen (O) moieties. The proposed method demonstrated substantial analytical robustness, enabling the sorbent bead to detect low concentrations of TCs, with limit of detection values ranging from 142 to 303 µg L^{-1}. Notably, the established linear range of 450−2000 µg L^{-1} extended the applicability of this approach to food and pharmaceutical product analysis. This study anticipated a paradigm shift in sample pre-treatment methodologies for TC analysis and envisions CS/Fe@PDA beads as a valuable tool for further advancements in separation science. The proposed bio-sorbent introduced a promising avenue for optimizing TC analysis, contributing to broader goals of food safety and pharmaceutical quality assurance. The results and insights from this study are expected to provide valuable inputs for ongoing efforts of the Food and Drug Administration to enhance analytical methodologies for food and drug safety.

Keywords: Bio-sorbent, Chitosan, Nanoparticle, Polydopamine, Tetracycline

1. Introduction

Tetracycline (TC) is the second most widely used antibiotic globally [1,2], playing a crucial role in combating various infections owing to its broad-spectrum activity against gram-positive and gram-negative bacteria, mycoplasma, fungi, Rickettsia, and parasites [3,4]. However, current methods for identifying antibiotic residues, including immunoassays [5] and biosensors [6], often lack specificity, struggle to differentiate between members of a particular antibiotic class.

Challenges arise in the identification of antibiotic residues because of their complex matrix environments [7,8]. Methods involving acid hydrolysis have been reported to decompose acid-sensitive antibiotics, prompting researchers to identify their alternatives [9−12]. Regulatory bodies, such as the Food and Drug Administration (FDA) and International Council for Harmonisation of Technical Requirements for

* Corresponding author.
E-mail address: yelihu@kmu.edu.tw (Y.-L. Huang).

Pharmaceuticals for Human Use ICH, have emphasized the application of experimental design approaches to chromatographic selectivity to enhance method control and transferability [13,14]. Consequently, researchers have incorporated experimental design principles into high-performance liquid chromatography (HPLC), resulting in the development of highly selective and sensitive methods [15−18].

Despite advancements in antibiotic analysis, challenges persists with extraction, cleanup, and pre-concentration of analytes from sample matrices [19−21]. Solid-phase extraction (SPE), a cost-effective sample preparation technique, has replaced traditional liquid−liquid extraction (LLE), owing to its high preconcentration factors, minimal organic solvent usage, and straightforward operation [22−24]. The composition of the adsorbent, which influences selectivity and sorptive capacity, is crucial for the SPE process [25−27]. Key considerations for extraction include adsorbent surface chemistry, porosity, and specific surface area. Ideally, an adsorbent should be biodegradable, sustainable, and non-toxic. Numerous materials, such as activated carbon [28], graphene oxide [29], metal-organic frameworks [30], polymeric resins [31], mesoporous/clay materials [32], biochar [33], and nanocomposites [34], have been explored for TC separation, but some may pose environmental risks or lack sensitivity and selectivity, underscoring the need to develop less hazardous, bio-based, and durable sorbents that can withstand diverse solvents during sample preparation.

In regions where substandard drugs, drug counterfeiting, and antibiotic-contaminated foods pose significant challenges, there is an urgent need for accurate, cost-effective, user-friendly, and rapid methods. These methods should utilize basic equipment to identify and quantify active components in complex formulations. Our study aims to address the limitations of existing HPLC methodologies for TC separation and determination. Although previous studies have contributed significantly, several challenges persist, including the lack of specificity in some approaches, potential decomposition of acid-sensitive antibiotics during sample preparation, and environmental impact of certain sorbents [11]. We introduced a novel approach that combines a less hazardous bio-based sorbent with experimental design principles for HPLC. The primary objective of this study is to develop and validate a new RP-HPLC method for accurate, linear, and sensitive TC estimation that is simple, reliable, and cost-effective, prioritizing environmental sustainability by using a biodegradable sorbent.

Our method involves the fabrication of sorbent chitosan (CS) bio-polymer beads incorporating poly-dopamine nanoparticles (PDA NPs) and Fe ions. The chitosan polycation and PDA NPs protect Fe from oxidation and facilitate smooth interaction between TC and Fe, ultimately leading to complex formation. Furthermore, the fabricated sorbent beads are seamlessly exhibiting significant extraction efficiency against four different TC antibiotics. Considering TC separation, determination, and recyclability, the proposed methodology, utilizing CS/Fe@PDA beads, was applied under real sample conditions, maintaining accuracy and robustness even after seven consecutive extraction and regeneration cycles during TC determination.

2. Materials and methods

2.1. Chemicals

High molecular weight Chitosan (CS) (Sigma−Aldrich, Iceland), 3-hydroxytyramine hydrochloride (Acros Organics, China), glutaraldehyde solution grade II 25% in H_2O (Sigma−Aldrich, Switzerland), $Fe(NO_3)_3$ standard solution (1000 mg L^{-1}, Merck KGaA, Darmstadt, Germany), oxalic acid 2-hydrate (Shimakyu's Pure Chemicals, Taiwan), oxytetracycline hydrochloride (Alfa Aesar, China), tetracycline hydrochloride (Calbichem, China), demeclocycline hydrochloride (Sigma−Aldrich, China), chlortetracycline hydrochloride (Thermo Scientific, China), acetonitrile (J.T. Baker, South Korea), and methyl alcohol anhydrous (Macron fine chemicals, Israel); all the above chemicals were procured as per above mentioned details. The TC standards were prepared using purified water with a resistivity of 18.2 MΩ·cm, and the same water was used to prepare all chemicals throughout the study (Thermo Scientific EDI system).

2.2. Instrumentation

The HPLC system (Jasco, Japan) was equipped with a HPLC pump (Jasco, PU-4180) and UV/visible detector (Jasco UV-2075) equipped with deuterium and halogen lamps from 190 to 600 nm. The chromatographic data were evaluated using the Clarity software provided by DataApex. Chromatographic separation was performed using a Phenomenex Luna 5u C18(2) 100A (250 × 4.6 mm, 5 μm) column. The pH values were measured using a SUNTEX SP-2100 pH meter (New Taipei, Taiwan). The samples were prepared using an elma transsonic digitals ultrasonic water bath (Singen am Hohentwiel, Germany). The analyte TC was eluted using an isocratic mode with a mobile phase composition of acetonitrile:

methanol:10 mM oxalic acid (20:10:70; pH 4.0) and a constant flow rate of 1.0 mL min^{-1} maintained throughout the analysis. The detector wavelength was 355 nm for TC molecules, and the injection volume was 20 μL for all determinations. Each day, the column was thoroughly eluted with any residual antibiotic by flushing with 50% methanol for 60 min. The peaks in the chromatograms were identified by comparison with the retention times and UV spectra of the standards. The peak area was used for quantification. All data were recorded under the chromatographic conditions described above. Fourier transform infrared (FTIR) spectra were recorded on a Bruker Optics-Alpha Opus spectrometer.

All solvents used in the chromatographic system were filtered through a 0.2 μm hydrophilic polypropylene membrane filter (PALL, Mexico) using a vacuum pump (GAST, MI, USA), and then degassed for 10 min in an ultrasonic bath.

2.3. Sorbent fabrication

To prepare PDA NPs, 10 mM of 3-hydroxytyramine hydrochloride (dopamine) and 10 mM of lysine were mixed with 50 mL of Tris−HCl buffer (pH 8.5) and vigorously stirred for 3 days to facilitate PDA NPs formation. In parallel, CS (2% w/v) was prepared by dispersing the required amount of CS powder in 50 mL of a 1000 mg L^{-1} Fe(NO$_3$)$_3$ standard solution using ultrasonication. Subsequently, the prepared PDA NPs were washed three times by centrifugation at 10,000 rpm for 20 min to remove the salt, and ultrapure water was used for redispersion at each step.

The resulting pellet was blended with the prepared chitosan mixture by ultrasonication to achieve homogeneity. Subsequently, the mixture was gradually added to the crosslinking solution to form adsorbent beads. The crosslinking solution was prepared by mixing 5.0 mL of 25% glutaraldehyde, 5.0 mL of a commercially available dishwasher (main ingredients: surfactant, citric acid, and NaOH), and 40 mL of ultrapure water. The surfactant in the dishwasher helps prevent bead aggregation, while citric acid and NaOH assist in cross-linking [35].

2.4. Sample preparation

Honey sourced from a local supermarket in Kaohsiung City, Taiwan, was used in this study. The sample was prepared by measuring 1.0 g of honey sample and diluting it to 10 mL with ultrapure water. Subsequently, the sample solutions underwent filtration through a 0.45 μm nylon filter to ensure purity. Subsequently, honey samples were spiked with the required quantity of TC to achieve the desired experimental conditions. For the commercial TC ointments, the preparation involved careful dilution to achieve the necessary concentrations. The ointments were diluted with ultrapure water to the predetermined concentration requirements. This simple, yet methodical procedure was adopted to maintain the integrity of the TC ointment samples, enabling a consistent and controlled approach for subsequent analyses.

2.5. Proposed analytical procedure

Initially, 3 mL of 1.0 μg mL^{-1} selected antibiotic mixture in 50% methanol solution (in water V/V) was treated with 0.1 g of prepared sorbent beads for 1 min without any pH adjustment. After the beads were transferred to a fresh tube, 3 mL of the eluent solvent, acetonitrile:methanol:oxalic acid (pH 4.0), was added and vortexed for 1 min, after which the elute was analyzed using an HPLC instrument at 355 nm.

3. Results and discussion

3.1. Sorbent fabrication and characterization

The separation bead is fabricated, as shown in Fig. 1. Initially, PDA was prepared by the oxidation and polymerization reaction at pH 8.5 and room temperature.

The CS/Fe blend was prepared by mixing the required amount of CS with Fe(NO$_3$)$_3$ in HNO$_3$ solution. Finally, the CS/Fe@PDA blend was prepared and crosslinked to produce the sorbent beads. An average size of the fabricated sorbent beads was approximately 2.75 ± 0.04 mm, and the fabricated beads are mostly consistent in size (Fig. 2A and B). The morphology of the fabricated, CS/Fe@PDA beads was examined using scanning electron microscope. The scanning electron microscopy (SEM) image shown in Fig. 2C reveals the nonporous and hollow crosslinked bead surface. After treatment with TC, no evident surface morphological changes are observed in sorbent beads (Fig. S1 (https://doi.org/10.38212/2224-6614.3510)), demonstrating the robustness of CS/Fe@PDA beads.

Furthermore, SEM-energy-dispersive X-ray spectroscopy (EDS) analysis shows that the CS/Fe@PDA beads exhibit the characteristic peaks of C, N, O, and Fe, which correspond to the precursors used (Fig. 2D). However, after TC treatment, some characteristic peak intensities tend to increase,
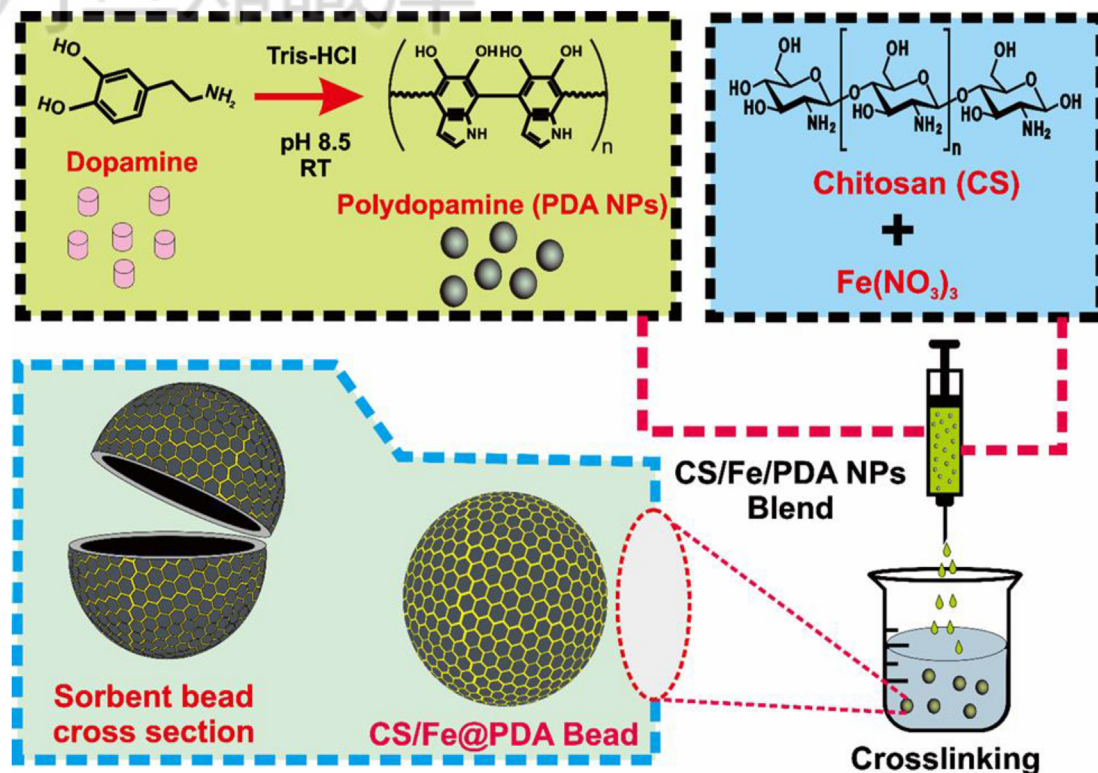
Fig. 1. Schematic representation of the steps involved in the fabrication of bio-based CS/Fe@PDA sorbent bead for tetracycline antibiotics (TCs) separation.
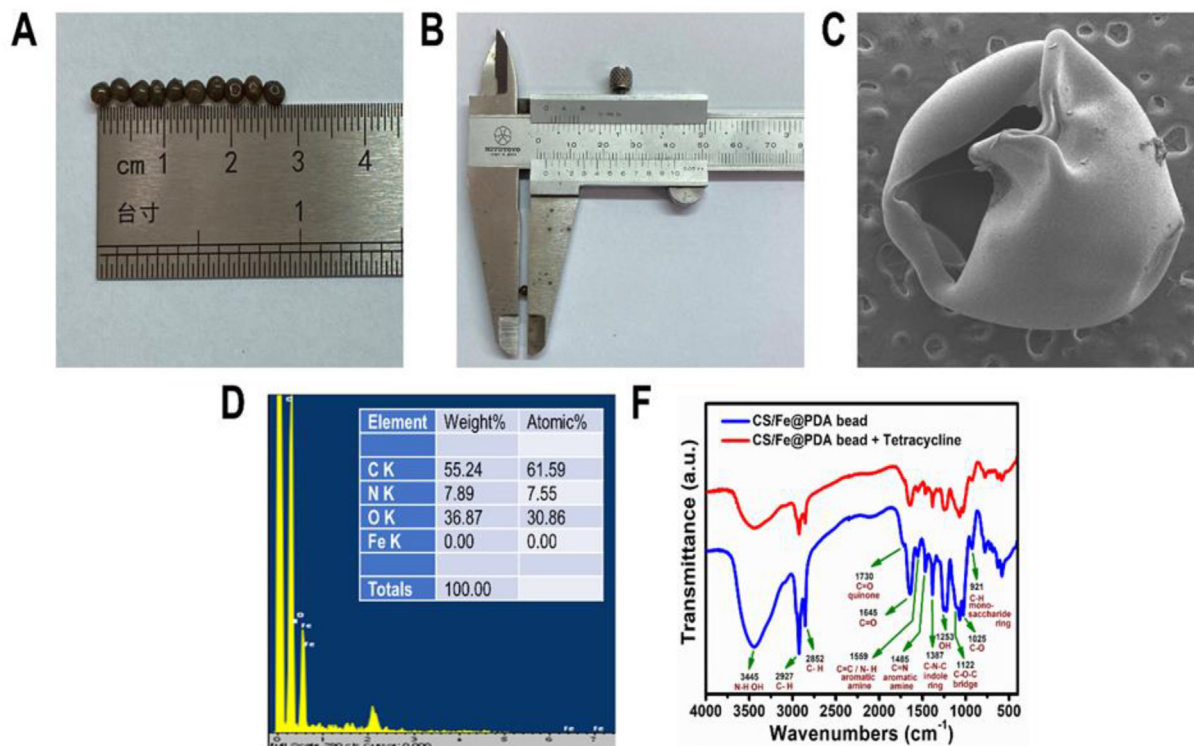

Fig. 2. Photographic (A & B) and scanning electron microscopy (SEM) images (C) depict the size and morphology of fabricated CS/Fe@PDA sorbent beads, respectively. SEM-energy-dispersive X-ray spectroscopy demonstrates the surface element presence on bead (D). Surface functional group changes of fabricated CS/Fe@PDA sorbent bead before and after TC separation are observed using Fourier transform infrared analysis (F).

attributable to TC integration on the bead surface (Fig. S2 (https://doi.org/10.38212/2224-6614.3510)). The characterization results indicate that the fabricated CS/Fe@PDA beads are robust and can successfully separate TC from aqueous samples.

3.2. FTIR analysis

The FTIR spectroscopy was conducted to explore the reaction-induced bond formation between chitosan (CS) and polydopamine (PDA) during cross-linking. The FTIR spectra obtained for the resulting CS/Fe@PDA beads exhibit characteristic peaks in the range of $400-3600$ cm^{-1} (Fig. 2F). Notably, the broadening of the band at 3445 cm^{-1} suggests the presence of intramolecular hydrogen bonding as well as OH and N–H stretching features characteristic of CS biopolymers, and is indicative of hydrogen bond formation between CS and PDA. Furthermore, the peaks at 2927 and 2852 cm^{-1} were identified as symmetric and asymmetric C–H stretching, respectively. The stretching absorbance bands at approximately 1730 and 1645 cm^{-1} indicated the presence of C=O (amide I) in PDA and CS, respectively. In addition, the peaks at 1559 and 1313 cm^{-1} were assigned to primary amine N–H bending and C–N stretching of amide III, respectively. The bands at 1426 and 1385 cm^{-1} confirmed the presence of CH_2 bending and CH_3 symmetrical deformation, respectively. The absorbance peak at 1253 cm^{-1} was attributed to the hydroxyl functional group in the CS biopolymer, whereas the asymmetric stretching peak at 1122 cm^{-1} indicated the presence of CS glycosidic bond (C–O–C) bridges. The weak stretching peak at 1025 cm^{-1} was attributed to the C–O bond, and the absorbance peak at 921 cm^{-1} was attributed to the C–H bending out of the CS monosaccharide ring plane. Notably, the FTIR spectra exhibited overlapping bands, corresponding to the PDA amide II, OH, N–H, and aromatic groups with similar groups in CS. These distinctive peaks underscored the key elements of the PDA nanoparticles, including the typical catechol and amine groups, confirming the successful oxidative polymerization of dopamine. The observed peaks below 600 cm^{-1} wavelength may be attributed to bond formation between Fe ions and O moieties present in CS and PDA. This observation confirmed the effective incorporation of Fe ions into the established CS/PDA networks. The obtained FTIR results aligned with those of previous reports on materials related to CS and PDA. These findings provide robust evidence supporting the hypothesis that hydrogen bonding and electrostatic interactions between CS and PDA contribute to the formation of

CS/PDA bead [36–39]. However, following TC treatment, the FTIR spectra of the CS/PDA beads exhibited a decrease in peak intensity at different locations. This finding clearly supports the integration of TC on the sorbent surface through a variety of interactions, including the metal chelation interaction between Fe and the TC analyte and $\pi-\pi$ interactions with PDA.

3.3. Analytical performance optimization

To effectively separate the target analyte, it is crucial to optimize the reaction conditions for the fabricated CS/Fe@PDA beads. The fabricated beads were challenged against various separation-influencing factors, including the effects of pH, contact time, and eluent type.

3.3.1. Influence of pH and contact time
TC exists as cationic, zwitterionic, and anionic species in acidic, moderately acidic to neutral, and alkaline conditions, respectively. The fabricated CS/Fe@PDA beads were treated with a fixed TC volume (3.0 mL) and concentration (1000 $\mu g\ L^{-1}$), but under varying pH reaction condition (4.0, 6.0, 8.0, 10.0, and 12.0). To ensure the stability of the pH levels during adjustments, we used a citrate and carbonate buffer system. The lowest pH 2.0 was omitted because it could disintegrate the beads by dissolving the CS. The resulting solution was analyzed through HPLC under a optimized conditions.

The results obtained from the study reveal that all the pH values exhibit significant extraction efficiency, which further indicates that the TC separation process by the CS/Fe@PDA beads is pH-independent (Figs. 3 and 4A). The utilized Fe ions tend to undergo oxidation under different pH conditions; however, the results suggest that the interaction between Fe ions and TC is not hindered by pH conditions. Furthermore, the amine functional groups from CS and PDA appear to act as protective agents for Fe ions against O moieties and water because the amine groups are strongly reactive with metal ions owing to their nitrogen atoms [40,41]. Previous studies have indicated the formation of stronger coordinate bonds between TC and Fe. TC contains multiple potential iron-binding sites, including the enolic oxygen at C3, amine nitrogen at C4 of the carboxamide group in ring A, and oxygen atoms in the C10–C12 phenolic diketone system. Interactions between TC and Fe^{3+} ions are anticipated to exhibit a complex pH-dependence, which is attributed to the presence of multiple ionizable functional groups in TC, characterized by the following pKa values: pKa1 = 3.3 (tricarbonylamide),
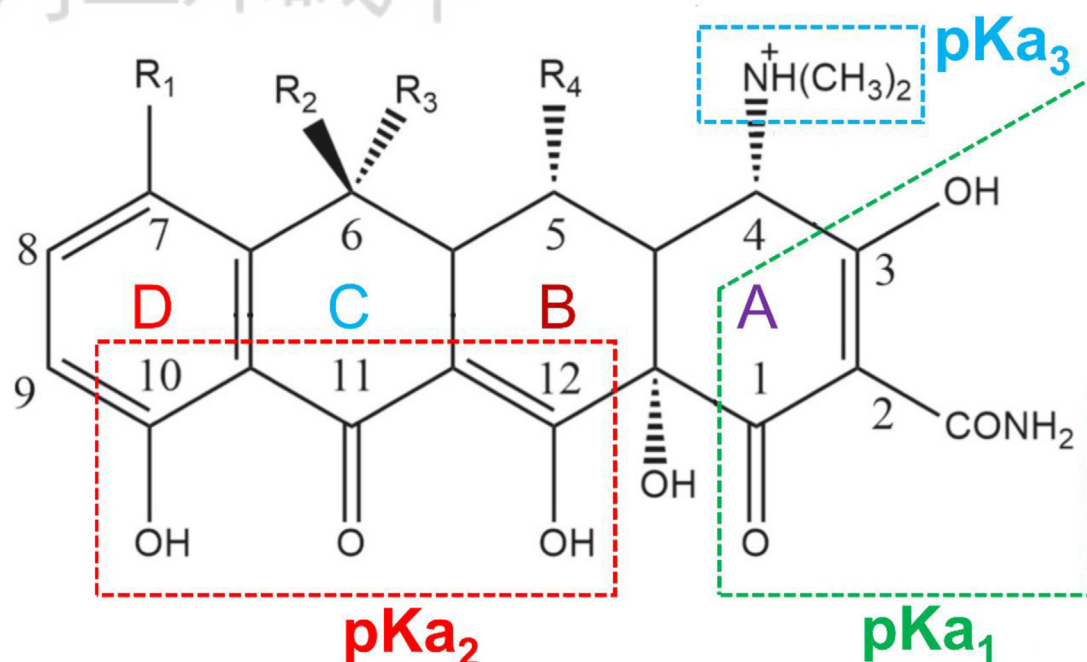
Type of TC antibiotics	R1	R2	R3	R4	pKa1, 2 & 3
Oxytetracycline	H	CH_3	OH	OH	3.2, 7.4, 8.9
Tetracycline	H	CH_3	OH	H	3.3, 7.7, 9.5
Demeclocycline	Cl	H	OH	H	3.3, 7.2, 9.3
Chlortetracycline	Cl	CH_3	OH	H	3.3, 7.5, 9.3

Fig. 3. Chemical Structures and pKa values of different type of tetracycline antibiotics.

pKa2 = 7.7 (phenolic diketone), and pKa3 = 9.5 (dimethylamine) [42], along with changes in the solubility/availability of Fe^{3+} at varying pH levels. In aqueous environments with pH above 5, the predominant form of Fe^{3+} is $Fe(OH)_3$, which is insoluble. In contrast, below this pH threshold, soluble hydroxyl complexes were present, with free (hexaaqua) Fe^{3+} prevailing below 2.0 pH levels. This finding suggests that the CS/Fe@PDA sorbent beads can be effectively used for samples across a wide pH range. These observations indicated that despite the notable electrostatic interaction between TC and CS/Fe@PDA beads, a substantial non-electrostatic interaction also exists, such as possible $\pi-\pi$ interactions between PDA and TC [43].

Contact time, a crucial factor in analyte separation, can be described as the maximum amount of analyte transferred from the aqueous phase to the sorbent surface at a defined time. If the sorbent produced significant extraction efficiency within a short contact time, it is considered efficient and tend to reduce the sample preparation time. As solid-phase extraction is an exhaustive technique, sufficient time is required to reach equilibrium. The contact time study was performed by treating the 0.1 g of sorbent bead (1.0 mg L^{-1}) with TC for different reaction times. The results shown in Fig. 4B and C reveal that for a contact time of 1.0 min, the CS/Fe@PDA beads can effectively adsorb more than 80% of the analyte. This finding evidently supports
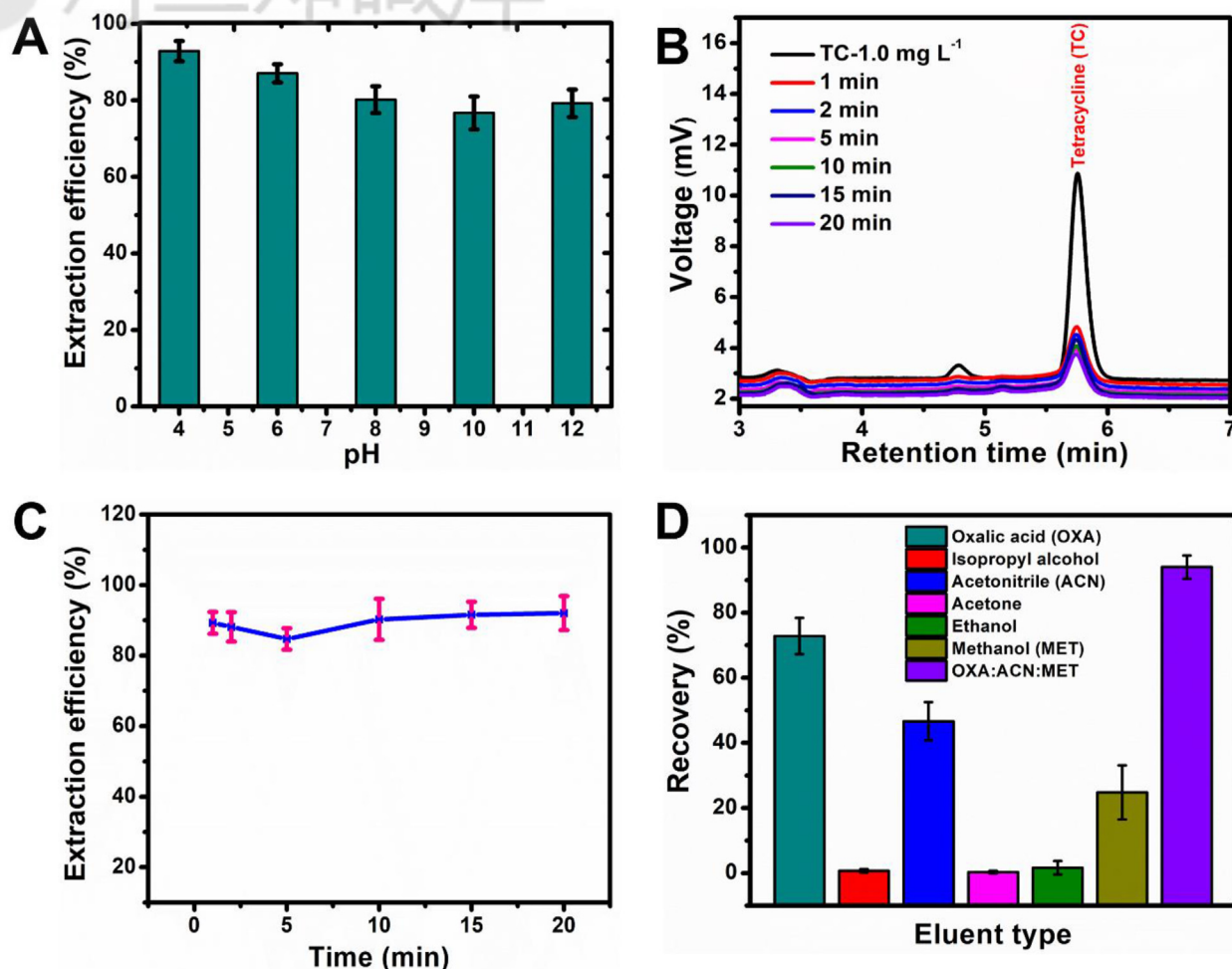
Fig. 4. Impact of reaction pH (A), sorbent contact time with analyte (B & C), and different eluent types (D) on the separation and quantification of the TC analyte (n = 3).

the significance of the fabricated sorbent considering the extraction efficiency percentage (%), based on the results throughout the experiment with 1.0 min as the contact time.

$$Extraction\ efficiency\ (\%) = A/B \times 100 \qquad (1)$$

where A is the recovered analyte concentration and B is used (starting) analyte concentration.

3.3.2. Eluent type

The efficiency of the extraction process is intricately linked to careful selection of the desorption solvent. Therefore, a desorption solvent must fulfill several critical criteria, including transparency across the necessary wavelength range, ability to dissolve target analytes, high affinity for the target compounds, and fast kinetics to ensure quantitative recovery within a short timeframe. To investigate the effective extraction of TC from the CS/Fe@PDA bead surface, various desorption solvents were systematically selected and used. These solvents were oxalic acid (OXA), isopropyl alcohol, acetonitrile (ACN), acetone, ethanol, methanol (MET), and a combination of oxalic acid, acetonitrile, and methanol in a ratio of 70:20:10 (OXA:ACN:MET). CS/Fe@PDA beads were treated with each desorption solvent for 5 min, followed by TC extraction. As shown in Fig. 4D, oxalic acid, acetonitrile, and methanol exhibit satisfactory recovery percentages (%) (Eq. (2)) individually. The combined use of oxalic acid, acetonitrile, and methanol synergistically improved recovery%. The superior elution efficiency of oxalic acid can be rationalized by its robust masking ability towards Fe ions, as corroborated by previous studies [44,45].

In contrast, the intricate $\pi-\pi$ interactions between TCs and acetonitrile revealed potent interactions [46], suggesting that acetonitrile exhibited enhanced efficacy in dissolving TCs than methanol. The interactions between the solvent and TC contributed

to the improved recovery percentage compared to other solvents, providing valuable insights contributed into the solvent-specific interactions that govern extraction efficiency. The careful selection of desorption solvents is crucial in optimizing the extraction efficiency of TC from CS/Fe@PDA beads. The observed synergies and specific interactions with solvents, particularly the unique contributions of oxalic acid and acetonitrile, provide valuable insights into the refinement of extraction protocols targeting TCs. Meticulous solvent selection is integral for developing robust methodologies for the extraction and recovery of target compounds for real-world analytical applications.

$$\text{Recovery percentage } (\%) = C_s - C_t/C_k \times 100 \qquad (2)$$

where, C_k is the known spiked sample concentration, C_t is the TC concentration of the blank target sample, and C_s is the TC concentration in the spiked sample.

3.4. Sensitivity of the proposed approach

Validation of the proposed analytical method involved a comprehensive examination of various performance parameters to ensure its reliability and accuracy under optimal experimental conditions. Among these parameters, linearity, coefficient of determination (R^2), limit of detection (LOD), limit of quantitation (LOQ), precision, and accuracy were evaluated. To assess linearity, calibration curves are accurately plotted by recording peak areas (y) against standard solution concentrations (x, mg L^{-1}) at certain distinct concentration levels spanning the range, as summarized in Table S1 (https://doi.org/10.38212/2224-6614.3510). This process was performed

for different TCs, namely oxytetracycline (Oxy), tetracycline (Tet), demeclocycline (Dem), and chlortetracycline (Chl). The resulting calibration curves exhibit R^2 values in the range of 0.996−0.998 for all the TCs, indicating a remarkably high degree of linearity and reliability (Fig. 5A). The assessment of the LOD and LOQ further highlighted the sensitivity of the method. The LOD and LOQ were calculated based on the signal-to-noise ratios of 3 and 10, respectively. The LOD values, ranging from 142 to 303 μg L^{-1}, signify the method's ability to detect trace amounts of TCs. The LOQ values, falling within the range of 425−939 μg L^{-1}, establish the method's ability to quantify these antibiotics at low concentrations (Table S1 (https://doi.org/10.38212/2224-6614.3510)). Notably, these results highlight the versatility of the proposed approach compared to the previously reported TC determination methods (Table 1), enabling the sensitive detection of four different types of TCs across a spectrum of concentrations. Moreover, it is exceedingly uncommon for all of the specified TCs to be found in honey samples. However, it is feasible to distinguish between the different types of TCs based on their observed retention times (RT): 5.06 min (Oxy), 5.77 min (Tet), 7.76 min (Dem), and 11.73 min (Chl), under the abovementioned HPLC conditions. This difference may be attributed to differences in their chemical structures, which result in distinct hydrophobic properties (Fig. S3 (https://doi.org/10.38212/2224-6614.3510)) [31].

Furthermore, the method's practical applicability was emphasized by obtaining a linear range and aligning it with the reported TC concentration in real samples, such as honey (920 μg L^{-1}) [50]. The linearity, LOD, and LOQ established the robustness and practical utility of the proposed analytical
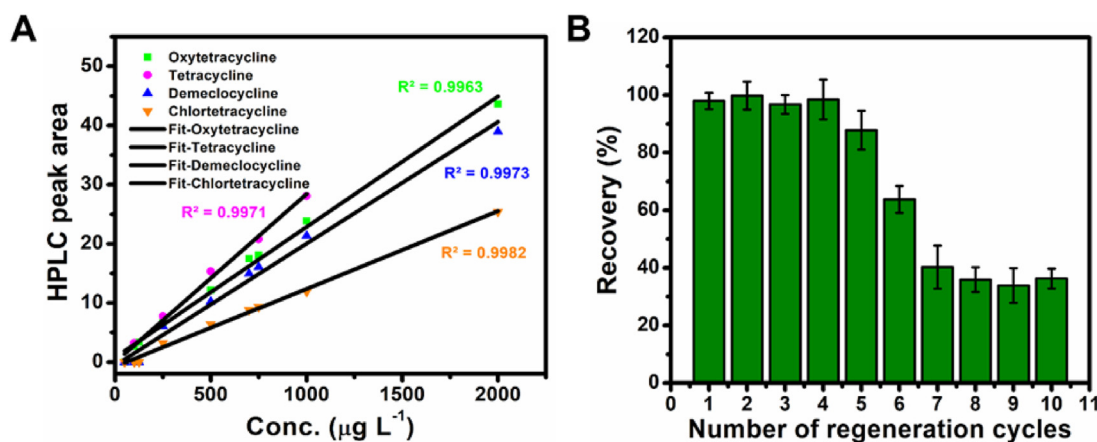

Fig. 5. Proposed method reveals significant linear dependency between various TC types concentration against area under the curve (A) and good sustainability nature in terms of regeneration (B) (n = 3).

Table 1. Efficiency of CS/Fe@PDA bead methodology in comparison to alternative techniques for HPLC-based various types of TC separation and determination (n = 3).

Sample preparation	Analytical method	Analyte	LOD ($\mu g\ L^{-1}$)	Reference
E-tongue	Electrochemical	Tetracycline	~ 300	[47]
UiO-66-NH$_2$	Fluorescent	Tetracycline	~ 199	[48]
Carbon dot	Förster resonance energy transfer	Oxytetracycline	~ 190	[49]
CS/Fe@PDA bead	HPLC	Oxytetracycline	190	This Study
CS/Fe@PDA bead	HPLC	Tetracycline	142	This Study
CS/Fe@PDA bead	HPLC	Demeclocycline	303	This Study
CS/Fe@PDA bead	HPLC	Chlortetracycline	257	This Study

Table 2. Assessment of various TC extraction and determination in honey samples using CS/Fe@PDA bead methodology (n = 3).

TC type	Spiked ($\mu g\ L^{-1}$)	Found ($\mu g\ L^{-1}$)	Recovery (%)	RSD (%)
Oxy	0	ND*	—	—
	600	624.7	104.1	3.2
	1000	968.4	96.8	5.6
	1500	1511.1	100.7	4.7
Tet	0	ND*	—	—
	500	507.7	101.5	1.9
	700	741.5	105.9	6.2
	900	852.3	94.7	4.9
Chl	0	ND*	—	—
	800	843.8	105.5	2.1
	1000	1024.2	102.4	5.6
	1500	1441.3	96.08	2.9

* ND = Not Detected.

method for accurate and sensitive detection of various TCs. The performance characteristics of the method make it a valuable tool for analytical applications in regulatory compliance and environmental monitoring.

3.5. Analytical performance of the approach

To evaluate the practical effectiveness of the proposed methodology, the CS/Fe@PDA bead sorbent was systematically tested using commercially obtained tea and TC ointment samples. The study utilizes honey sample that was spiked with three discrete concentrations of TC, as summarized in Table 2, to mimic real situations. For the preparation of various TC ointments, a straightforward dilution procedure was employed, utilizing methanol at a concentration of 50% v/v. This resulted in the creation of three distinct concentrations of TC's as outlined in Table 3, these concentrations were strategically selected to replicate the conditions encountered in real-world scenarios. Subsequently, the CS/Fe@PDA bead sorbent was used to treat honey and ointment samples under carefully optimized reaction conditions. The results summarized in Tables 2 and 3 signify that the proposed sample preparation method demonstrated remarkable recovery values ranging between 92% and 105%, for all samples. This finding underscores the effectiveness of the method for selectively extracting TCs, mitigating potential interference from the non-specific adsorption of other compounds, such as commercial ointments.

The proposed method was tested for accuracy using a 3.0 mL of carefully selected concentration of TCs under ideal reaction conditions. After extraction and desorption, HPLC analysis was performed on

Table 3. Analytical proficiency of the CS/Fe@PDA bead approach for various TC extraction and quantification in different commercial TC ointments (n = 3).

Sample	Diluted ($\mu g\ L^{-1}$)	Found ($\mu g\ L^{-1}$)	Recovery (%)	RSD (%)
Commercial tetracycline Ointment (10 mg g^{-1})	0	ND*	—	—
	500	518.4	103.6	7.04
	700	691.8	98.8	5.3
	900	908.1	100.9	6.5
Commercial Chlortetracycline ointment-1 (10 mg g^{-1})	0	ND*	—	—
	800	820.6	102.5	6.8
	1000	1017.6	101.8	2.7
	1500	1388.7	92.6	2.3
Commercial Chlortetracycline ointments-2 (30 mg g^{-1})	0	ND*	—	—
	800	826.6	103.3	4.4
	1000	1006.5	100.7	1.01
	1500	1482.7	98.8	5.3

* ND = Not Detected.

Table 4. Evaluating accuracy of the proposed method in TC extraction and determination.

Sample	Intraday (n = 5)				Interday (n = 5)		
	Spiked/Diluted (μg L^{-1})*	Found (μg L^{-1})	Recovery (%)	RSD (%)	Found (μg L^{-1})	Recovery (%)	RSD (%)
Honey + Oxytetracycline	1000	1009.2	100.9	4.8	927.2	92.7	6.4
Commercial tetracycline Ointment (10 mg g^{-1})	700	732.9	104.7	2.5	724.3	103.5	4.8
Honey + Demeclocycline	1200	1183.05	98.6	5.07	1172.3	97.7	6.7
Commercial Chlortetracycline ointment-1 (10 mg g^{-1})	1000	998.6	99.8	1.5	947.5	94.7	8.7

* The required amount of TC was spiked into the honey samples, whereas commercial TC ointments were diluted to achieve the necessary concentration.

the resulting solutions. The acquired data revealed acceptable relative standard deviation (RSD%) values in the range of 1.59−5.07 for all samples summarized in Table 4, indicating precise intraday accuracy. Moreover, the interday accuracy experiment yielded noteworthy RSD% values ranging from 4.86 to 8.7 for all samples. These findings affirm that the proposed method exhibits not only robust inter-and intraday precision for the selected TCs, but also fulfills the criteria for reliability and feasibility, supporting its suitability of for enhanced analysis of real-world samples.

3.6. Reusability

The reusability of an adsorbent is critical for its practical viability in commercial applications, thus emphasizing the sustainability of the proposed methodology. To thoroughly evaluate this aspect, the proposed approach was meticulously tested over 10 cycles of TC extraction and desorption. Notably, the methodology exhibited remarkable reusability, attaining recovery values within the acceptable range of 85%−115% for TC across five consecutive cycles, demonstrating sustained analytical performance. This behavior underscores the robust nature of the engineered CS/Fe@PDA beads. The CS networks weaken and solubilize under acidic conditions. However, the glutaraldehyde cross-linking yielded notable acid-resistant properties in the resulting sorbent beads, enabling five exceptional cycles of regeneration and reuse. The observed decline in the recovery% values after five cycles may be attributed to potential loss of Fe ions, and the CS/PDA presenting active sites during the acid-based sorbent regeneration process. This phenomenon can reduce the availability of active sites, hindering efficient TC extraction. Understanding the factors that influence the reusability of the proposed approach is crucial for sustained and effective TC extraction and determination in successive cycles (Fig. 5B).

4. Conclusion

In conclusion, we introduced a highly efficient strategy for the pre-concentration and simultaneous determination of four TCs in aqueous samples. This analytical approach, which integrates a bio-sorbent based methodology with HPLC, is simple, expeditious, accurate, selective, and effective. The analytical performance results confirmed the potential of the engineered CS/Fe@PDA beads as a viable and efficient tool for sample pre-treatment in the pre-concentration and RPLC determination of TCs. Our proposed method exhibits distinct advantages over existing approaches, considering the sample preparation time, nontoxicity, and degradability. The fabricated CS/Fe@PDA beads exhibited an impressive ability to effectively extract over 80% of the TCs within a minute. Our findings not only improve the analysis of TCs, but also pave the way for innovative possibilities and future advancements in separation science. The positive outcomes of this study not only improve the analysis of TC, but also open up new possibilities for improving sample-pretreatment methodologies. We anticipate that the versatility and efficacy demonstrated by our fabricated bio-sorbent will inspire further developments in environmental and pharmaceutical research.

Conflict of interest statement

The authors declare that they have no competing of interests.

CRediT authorship contribution statement

Emmanuvel Arputharaj: Conceptualization, Investigation, Methodology, Formal analysis, Validation, Data curation, Writing - Original Draft, Writing - Review & Editing. Yu-Hui Huang: Experiment, Data curation, Formal analysis. Shivangi Singh: Formal analysis. Chen-Han Zhuang: Experiment, Formal analysis. Kuei-Ying Lin: Formal

ORIGINAL ARTICLE

References

[1] Leichtweis J, Vieira Y, Welter N, Silvestri S, Dotto GL, Carissimi E. A review of the occurrence, disposal, determination, toxicity and remediation technologies of the tetracycline antibiotic. Process Saf Environ Protect 2022;160:25—40.

[2] Taylor P, Reeder R. Antibiotic use on crops in low and middle-income countries based on recommendations made by agricultural advisors. CABI Agric Biosci 2020;1:1.

[3] Lugarini C, Silva LTR, de Amorim MMR, de Lima DCV, Santos SB, Saidenberg AB, et al. Free-living birds from caatinga and atlantic forest of northeast Brazil as hosts of enterobacterales spp. Ornithol Res 2021;29:149—59.

[4] Chao H, Sun M, Ye M, Zheng X, Hu F. World within world: intestinal bacteria combining physiological parameters to investigate the response of Metaphire guillelmi to tetracycline stress. Environ Pollut 2020;261:114174.

[5] Li Y, Wang J, Tian Y, Huang Z, Qian C, Duan Y. The development of a wash-free homogeneous immunoassay method for the detection of tetracycline in environmental samples. Analyst 2021;146:4918—26.

[6] Wang YL, Sun YJ, Dai HC, Ni PJ, Jiang S, Lu WD, et al. A colorimetric biosensor using Fe_3O_4 nanoparticles for highly sensitive and selective detection of tetracyclines. Sens Actuators B: Chem 2016;236:621—6.

[7] Liu XG, Huang DL, Lai C, Zeng GM, Qin L, Zhang C, et al. Recent advances in sensors for tetracycline antibiotics and their applications. Trac-Trend Anal Chem 2018;109:260—74.

[8] El Alami El Hassani N, Baraket A, Boudjaoui S, Taveira Tenorio Neto E, Bausells J, El Bari N, et al. Development and application of a novel electrochemical immunosensor for tetracycline screening in honey using a fully integrated electrochemical Bio-MEMS. Biosens Bioelectron 2019;130:330—7.

[9] Moorthy K, Chang KC, Yang HH, Su WM, Chiang CK, Yuan Z. Recent developments in detection and therapeutic approaches for antibiotic-resistant bacterial infections. J Food Drug Anal 2023;31:1—19.

[10] Biswas AK, Rao GS, Kondaiah N, Anjaneyulu ASR, Mendiratta SK, Prasad R, et al. A simple multi-residue method for determination of oxytetracycline, tetracycline and chlortetracycline in export buffalo meat by HPLC-photodiode array detector. J Food Drug Anal 2007;15:278—84.

[11] Zhang Y, Li XQ, Li HM, Zhang QH, Gao Y, Li XJ. Antibiotic residues in honey: a review on analytical methods by liquid chromatography tandem mass spectrometry. Trac-Trend Anal Chem 2019;110:344—56.

[12] Arabsorkhi B, Sereshti H. Determination of tetracycline and cefotaxime residues in honey by micro solid phase extraction based on electrospun nanofibers coupled with HPLC. Microchem J 2018;140:241—7.

[13] Patel MN, Kothari CS. Review on implementation of multivariate approach for forced degradation study and impurity profiling with regulatory considerations. Chromatographia 2018;81:105—25.

[14] Tome T, Zigart N, Casar Z, Obreza A. Development and optimization of liquid chromatography analytical methods by using AQbD principles: overview and recent advances. Org Process Res Dev 2019;23:1784—802.

[15] Agadellis E, Tartaglia A, Locatelli M, Kabir A, Furton KG, Samanidou V. Mixed-mode fabric phase sorptive extraction of multiple tetracycline residues from milk samples prior to high performance liquid chromatography-ultraviolet analysis. Microchem J 2020;159:105437.

[16] Al-Afy N, Sereshti H, Hijazi A, Rashidi Nodeh H. Determination of three tetracyclines in bovine milk using magnetic solid phase extraction in tandem with dispersive liquid-liquid microextraction coupled with HPLC. J Chromatogr, B: Anal Technol Biomed Life Sci 2018;1092:480—8.

[17] Feng MX, Wang GN, Yang K, Liu HZ, Wang JP. Molecularly imprinted polymer-high performance liquid chromatography for the determination of tetracycline drugs in animal derived foods. Food Control 2016;69:171—6.

[18] Rama A, Lucatello L, Benetti C, Galina G, Bajraktari D. Assessment of antibacterial drug residues in milk for consumption in Kosovo. J Food Drug Anal 2017;25:525—32.

[19] Tang S, Zhang H, Lee HK. Advances in sample extraction. Anal Chem 2016;88:228—49.

[20] Kanu AB. Recent developments in sample preparation techniques combined with high-performance liquid chromatography: a critical review. J Chromatogr A 2021;1654:462444.

[21] Li LN, Chen YL, Yang L, Wang ZT, Liu HW. Recent advances in applications of metal-organic frameworks for sample preparation in pharmaceutical analysis. Coord Chem Rev 2020;411:213235.

[22] Wan QQ, Liu H, Deng ZW, Bu JQ, Li TH, Yang YJ, et al. A critical review of molecularly imprinted solid phase extraction technology. J Polym Res 2021;28:401.

[23] Płotka-Wasylka J, Szczepańska N, de la Guardia M, Namieśnik J. Miniaturized solid-phase extraction techniques. TrAC, Trends Anal Chem 2015;73:19—38.

[24] Faraji M, Yamini Y, Gholami M. Recent advances and trends in applications of solid-phase extraction techniques in food and environmental analysis. Chromatographia 2019;82:1207—49.

[25] Aguilar JFF, Miranda JM, Rodriguez JA, Paez-Hernandez ME, Ibarra IS. Selective removal of tetracycline residue in milk samples using a molecularly imprinted polymer. J Polym Res 2020;27:176.

[26] Effting LM, Urbano A, do Lago AC, de Figueiredo EC, Tarley CRT. Synthesis of novel oxytetracycline-molecularly imprinted polymer using a semi-covalent chemical imprinting approach for magnetic dispersive solid phase extraction of tetracyclines in water and milk samples. Food Chem 2024;437(Pt 2):137854.

[27] Zeng GL, Liu YY, Ma XG, Fan YM. Fabrication of magnetic multi-template molecularly imprinted polymer composite for the selective and efficient removal of tetracyclines from water. Front Environ Sci Eng 2021;15:107.

[28] Martins AC, Pezoti O, Cazetta AL, Bedin KC, Yamazaki DAS, Bandoch GFG, et al. Removal of tetracycline by NaOH-activated carbon produced from macadamia nut shells: kinetic and equilibrium studies. Chem Eng J 2015;260:291−9.

[29] Wang JH, Liu RH, Yin XL. Adsorptive removal of tetracycline on graphene oxide loaded with titanium dioxide composites and photocatalytic regeneration of the adsorbents. J Chem Eng Data 2018;63:409−16.

[30] Yang ZH, Cao J, Chen YP, Li X, Xiong WP, Zhou YY, et al. Mn-doped zirconium metal-organic framework as an effective adsorbent for removal of tetracycline and Cr(VI) from aqueous solution. Microporous Mesoporous Mater 2019;277:277−85.

[31] Yang WB, Zheng FF, Lu YP, Xue XX, Li N. Adsorption interaction of tetracyclines with porous synthetic resins. Ind Eng Chem Res 2011;50:13892−8.

[32] Gopal G, Alex SA, Chandrasekaran N, Mukherjee A. A review on tetracycline removal from aqueous systems by advanced treatment techniques. RSC Adv 2020;10:27081−95.

[33] Dai Y, Li J, Shan D. Adsorption of tetracycline in aqueous solution by biochar derived from waste Auricularia auricula dregs. Chemosphere 2020;238:124432.

[34] Ahamad T, Naushad M, Al-Shahrani T, Al-Hokbany N, Alshehri SM. Preparation of chitosan based magnetic nanocomposite for tetracycline adsorption: kinetic and thermodynamic studies. Int J Biol Macromol 2020;147:258−67.

[35] Sedyakina NE, Zakharov AN, Krivoshchepov AF, Pribytkova AP, Bogdanova YA, Feldman NB, et al. Effect of carbon chain length of dicarboxylic acids as cross-linking agents on morphology, encapsulation, and release features of protein-loaded chitosan microparticles. Colloid Polym Sci 2017;295:1915−24.

[36] Wang TR, Wusigale Kuttappan D, Amalaradjou MA, Luo YG, Luo YC. Polydopamine-coated chitosan hydrogel beads for synthesis and immobilization of silver nanoparticles to simultaneously enhance antimicrobial activity and adsorption kinetics. Adv Compos Hybrid Mater 2021;4:696−706.

[37] Wang Y, Zhang Y, Hou C, Liu MZ. Mussel-inspired synthesis of magnetic polydopamine-chitosan nanoparticles as biosorbent for dyes and metals removal. J Taiwan Inst Chem Eng 2016;61:292−8.

[38] Zheng R, Wang S, Tian Y, Jiang X, Fu D, Shen S, et al. Polydopamine-coated magnetic composite particles with an enhanced photothermal effect. ACS Appl Mater Interfaces 2015;7:15876−84.

[39] Yu X, Fan H, Liu Y, Shi Z, Jin Z. Characterization of carbonized polydopamine nanoparticles suggests ordered supramolecular structure of polydopamine. Langmuir 2014;30:5497−505.

[40] Wang JL, Zhuang ST. Removal of various pollutants from water and wastewater by modified chitosan adsorbents. Crit Rev Environ Sci Technol 2017;47:2331−86.

[41] Assa F, Jafarizadeh-Malmiri H, Ajamein H, Vaghari H, Anarjan N, Ahmadi O, et al. Chitosan magnetic nanoparticles for drug delivery systems. Crit Rev Biotechnol 2017;37:492−509.

[42] Korać Jačić J, Milenković MR, Bajuk-Bogdanović D, Stanković D, Dimitrijević M, Spasojević I. The impact of ferric iron and pH on photo-degradation of tetracycline in water. J Photochem Photobiol, A: Chem 2022;433:114155.

[43] Korać J, Stanković DM, Stanić M, Bajuk-Bogdanović D, Žižić M, Pristov JB, et al. Coordinate and redox interactions of epinephrine with ferric and ferrous iron at physiological pH. Sci Rep 2018;8:3530.

[44] Zhang J, Yang Y, Sun CJ, Wu L. Sample preparation and instrumental detection methods for tetracycline antibiotics. Int J Environ Anal Chem 2023:1−30.

[45] Yang Y, Yin S, Yang D, Jiang Y, Li Y, Zhou C, et al. Carboxyl Fe_3O_4 magnetic nanoparticle-based SPE and HPLC method for the determination of six tetracyclines in water. Anal Bioanal Chem 2019;411:507−15.

[46] Xu JJ, An M, Yang R, Tan Z, Hao J, Cao J, et al. Determination of tetracycline antibiotic residues in honey and milk by miniaturized solid phase extraction using chitosan-modified graphitized multiwalled carbon nanotubes. J Agric Food Chem 2016;64:2647−54.

[47] Scagion VP, Mercante LA, Sakamoto KY, Oliveira JE, Fonseca FJ, Mattoso LHC, et al. An electronic tongue based on conducting electrospun nanofibers for detecting tetracycline in milk samples. RSC Adv 2016;6:103740−6.

[48] Wang X, Wang X. UiO-66-NH_2 based fluorescent sensing for detection of tetracyclines in milk. RSC Adv 2022;12:23427−36.

[49] Fu Y, Huang L, Zhao S, Xing X, Lan M, Song X. A carbon dot-based fluorometric probe for oxytetracycline detection utilizing a Forster resonance energy transfer mechanism. Spectrochim Acta Mol Biomol Spectrosc 2021;246:118947.

[50] Yang Y, Lin G, Liu L, Lin T. Rapid determination of multi-antibiotic residues in honey based on modified QuEChERS method coupled with UPLC-MS/MS. Food Chem 2022;374:131733.